

Physical properties of $\text{Ga}_{0.03}\text{Zn}_{0.97}\text{O}$ thin film prepared by spray pyrolysis: Dependence on annealing temperature

Salam Amir Yousif¹, Sana Juma Ali²

^{1,2}Department of Physics, College of Education, the University of Mustansiriyah, Baghdad, Iraq

ABSTRACT

Gallium doped zinc oxide (GZO) thin film has been deposited by spray pyrolysis technique onto glass substrates. The Effect of annealing temperature on the structural, morphological and optical properties of $\text{Ga}_{0.03}\text{Zn}_{0.97}\text{O}$ thin film has been investigated. All the films are polycrystalline with a preferential c-axis (002) orientation. It is shown that the full width at half maximum (FWHM) value decreases from 0.4472 to 0.2717^o with increasing annealing temperature indicating the improvement of the crystalline quality of $\text{Ga}_{0.03}\text{Zn}_{0.97}\text{O}$ film. The surface morphology changed with the varying annealing temperatures. It is observed that, as the annealing temperature increased, the diffusion of atoms on the surface of glass substrate was enhanced, resulting in a flat or less rugged surface with (RMS) roughness 0.929 nm for the sample annealed at 450°C. Therefore it is concluded that the sufficient surface diffusion leads to the improvement of crystalline quality which accompanies the modification of the surface morphology. The as-deposited film was less transparent in the visible and IR regions than other annealed films and the transparency of the films improved as the annealing temperature increased up to 450°C and then it decreases for further increasing in annealing temperature at 500°C.

1. INTRODUCTION

ZnO is a II-VI semiconductor with a large band gap (approx. 3.4 eV) at room temperature and has large exciton binding energy (~60 meV) [1]. Wide-band gap oxide semiconductor for optical devices, liquid crystal displays, and solar cells have attracted much attention. ZnO has been a promising material for many different applications such as gas sensors [2], transparent electrodes [3], piezoelectric devices [4], varistors [5], and surface acoustic wave devices [6]. ZnO thin film is fabricated by several methods: sputtering [7], [8], reactive plasma deposition (RPD) [9], [10], pulsed laser deposition (PLD) [11], metal organic vapor phase epitaxy (MOVPE) [12] and spray pyrolysis [13], [14].

While synthesizing transparent conducting oxide (TCO) thin films, it is a common practice to introduce impurities such as In, Al, Ga, N, P, As and F [15], within ZnO thin films in order to enhance the optoelectronic properties. All the transparent conductive doped ZnO films provide excellent UV shielding due to the absorption edge on the short wavelength side ($\lambda \sim 300\text{nm}$) [16]. Beside, high reflectance in the IR region can make this a good candidate for application as the coating for IR reflecting mirror or heat reflector, as well as in other field of technology [17], [18]. All these applications require films with good uniformity, high electrical conductivity and high electron concentration simultaneously with high transmittance to visible light and high reflectance to near-IR light [19], [20]. From many reported investigations of the doped effect of impurity on ZnO, Ga doped seems to be the most successful and promising due to its advantages, such as the similar atomic radius compared to Zn, which could result in only small lattice deformation even for the case of high Ga concentrations [21], [22]. Also, Ga is less reactive and more resistive to oxidation compared to Al [23], [24]. Therefore, Ga doping can produce higher electron concentration than Al doping, which may be more useful for improving the reflective behavior of transparent conductive ZnO films according to Drude theory.

In this study, we fabricated and characterized $\text{Ga}_{0.03}\text{Zn}_{0.97}\text{O}$ single-layer film as the first step of the application mentioned above. Then, effect of annealing temperature on the several fundamental properties such as structural, morphological and optical properties of the obtained film has been investigated.

2. EXPERIMENTAL

The $\text{Ga}_{0.03}\text{Zn}_{0.97}\text{O}$ thin film was deposited by spray pyrolysis technique under ambient atmosphere. Two kinds of aqueous solutions, Zinc acetate $\text{Zn}(\text{CH}_3\text{COO})_2 \cdot 2\text{H}_2\text{O}$ and Gallium nitrate $\text{Ga}(\text{NO}_3)_3$, were chosen as the sources of zinc and gallium respectively. The concentration of the solutions was kept at 0.1M and a few drops of HCl were added to the solution to increase the solubility of the compounds. The $\text{Ga}_{0.03}\text{Zn}_{0.97}\text{O}$ film was prepared onto ultrasonically cleaned glass substrate held at a substrate temperature of 350°C. The substrate temperature was maintained constant using temperature controller with an accuracy of $\pm 10^\circ\text{C}$. The solution flow rate was fixed at 6ml/min. The samples were annealed under ambient atmosphere at 400, 450, 500 °C for 1hour.

The crystal structure of $\text{Ga}_{0.03}\text{Zn}_{0.97}\text{O}$ thin films was investigated by X-ray diffraction (XRD) using SHIMADZU X-Ray diffractometer system (XRD - 6000). The surface morphology of $\text{Ga}_{0.03}\text{Zn}_{0.97}\text{O}$ thin film has been examined by using atomic force microscopy (AFM, scanning probe microscope). The optical measurements of $\text{Ga}_{0.03}\text{Zn}_{0.97}\text{O}$ thin film is

calculated from the transmittance and absorbance spectrum at normal incidence over the range (300 – 900 nm), by using UV-VIS spectrophotometer type (SHIMADZU) (UV-1600/1700 series).

3. RESULTS AND DISCUSSION

3.1. STRUCTURAL PROPERTIES

The crystal orientation and crystallinity of the film was determined by X-ray diffraction. Figure 1 shows the XRD spectra of $\text{Ga}_{0.03}\text{Zn}_{0.97}\text{O}$ thin film as-deposited and annealed at 400, 450, 500 °C under ambient atmosphere. At as-deposited and all annealing temperature the films are polycrystalline with a preferential c-axis (002) orientation along with the other (101), (100) reflections that corresponding to the hexagonal wurtzite structure of ZnO. This is because the similar radii between the Zn^{2+} ions and Ga^{3+} ions enable the substitution of Ga for Zn without any significant change in the lattice constants of $\text{Ga}_{0.03}\text{Zn}_{0.97}\text{O}$ compared to those in ZnO. The observed d-values are presented in Table 1, and compared with the standard ones from the (JCPDS) data file (36-1451) [25]. This fact also indicates no change of the wurtzite structure, well-consist with other reports [26]-[30].

It is shown that the full width at half maximum (FWHM) value decreases from 0.4472 to 0.2717° with increasing annealing temperature indicating the improvement of the crystalline quality of $\text{Ga}_{0.03}\text{Zn}_{0.97}\text{O}$ film. The crystalline quality of the films depends strongly on the annealing temperature due to the enhanced surface diffusion that comes with increasing annealing temperature, which is consist with the report [31].

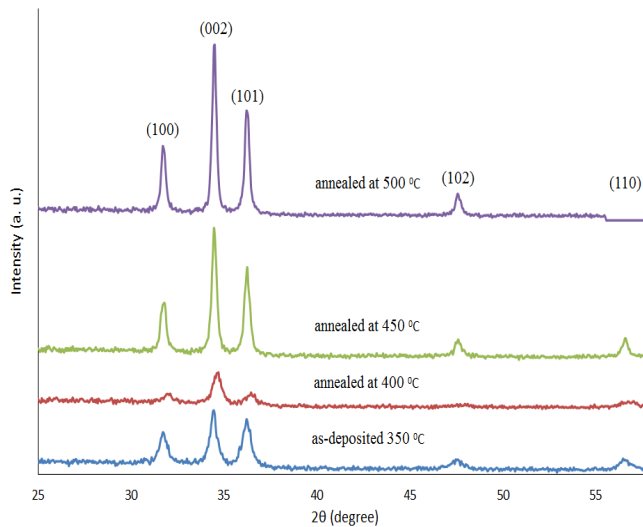


Figure 1 XRD pattern of $\text{Ga}_{0.03}\text{Zn}_{0.97}\text{O}$ thin film for different annealing temperature

Table1: XRD parameters of as-deposited and annealed $\text{Ga}_{0.03}\text{Zn}_{0.97}\text{O}$ thin film

Annealing Temperature °C		as-deposited	400	450	500	JCPDS for ZnO	
<i>(hkl)</i>	(100)	2θ(deg.)	31.739	31.742	31.751	31.753	31.77
		d(Å)	2.8169	2.8167	2.8159	2.8157	2.816
		Int.	58	56	40	40	57
	(002)	2θ(deg.)	34.437	34.455	34.482	34.485	34.422
		d(Å)	2.6021	2.6008	2.5989	2.5986	2.602
		Int.	100	100	100	100	44
	(101)	2θ(deg.)	36.214	36.214	36.241	36.242	36.253
		d(Å)	2.4784	2.4784	2.4766	2.4766	2.476
		Int.	88	84	67	65	100

The unit cell parameter (a, c) and the ratio of (c/a) belong to the (002) plane as a preferred orientation of $\text{Ga}_{0.03}\text{Zn}_{0.97}\text{O}$ thin films deposited on glass substrate have been calculated using equation (1) [32]. The calculated values of lattice parameter (a, c) and (c/a) are shown in Figures 2,3 and listed in Table 2, found to be in a good agreement with the standard (JCPDS) values [25].

$$\frac{1}{d^2} = \frac{4h^2 + hk + k^2}{3a^2} + \frac{l^2}{c^2} \quad (1)$$

Table 2: Lattice constants of $\text{Ga}_{0.03}\text{Zn}_{0.097}\text{O}$ thin film

annealing temperature °C	a (Å)	c (Å)	c/a
as-deposited (350)	3.25273	5.20434	1.5999
400	3.25247	5.20172	1.5993
450	3.25157	5.19786	1.5985
500	3.25137	5.19728	1.5984
(JCPDS)	3.24982	5.20661	1.6021

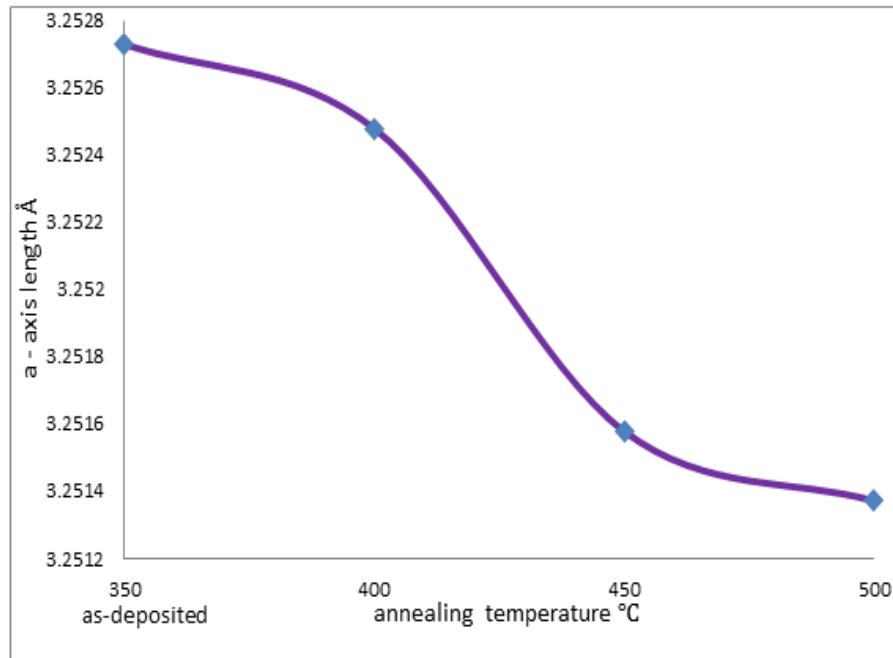


Figure 2 a-axis lengths vs. annealing temperature

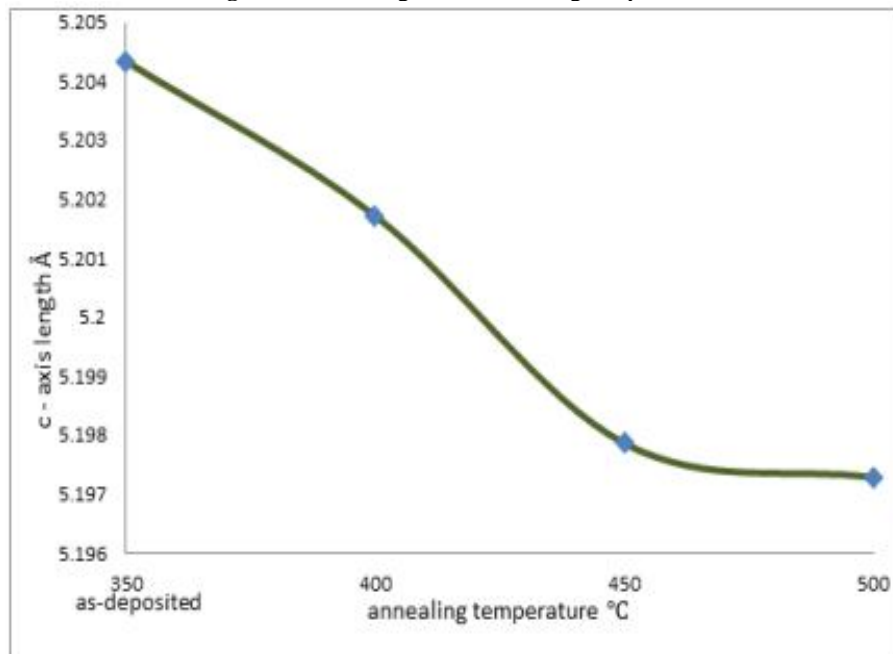


Figure 3 c-axis length vs. annealing temperature

The crystallite sizes of as-deposited and annealed $\text{Ga}_{0.03}\text{Zn}_{0.097}\text{O}$ thin films prepared on glass substrate are calculated using the full width at half maximum (FWHM) of (002) peak employing Scherer Formula equation (2)[33]. It can be noted that the value of crystallite size increases with increasing annealing temperature, because the crystallite size is

inversely proportional with the full width at half maximum. The values of crystallite size of $\text{Ga}_{0.03}\text{Zn}_{0.097}\text{O}$ thin films are shown in Figure 4, and listed in Table 3.

$$D = \frac{0.9\lambda}{\beta \cos \theta} \quad (2)$$

Where λ is the wavelength of X-ray used (1.5406 Å), β is the full-width at half maximum (FWHM) of the peak which has maximum intensity and θ is the Bragg angle.

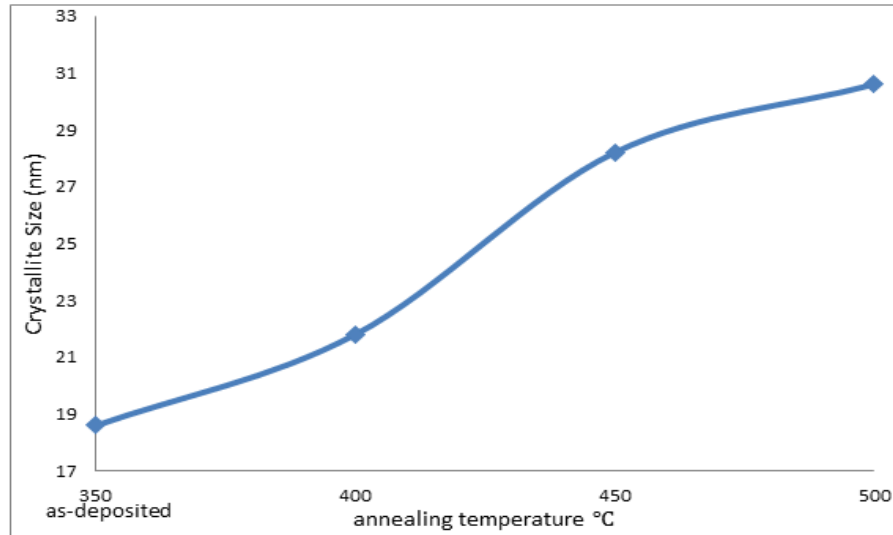


Figure 4 Crystallite size vs. annealing temperature

The texture coefficient (T_c) evaluated from equation (3) [33] is used to describe the preferred orientation of $\text{Ga}_{0.03}\text{Zn}_{0.097}\text{O}$ thin films. It is clear that the deviation of the texture coefficient from unity implies the preferred orientation of growth. The larger the texture coefficient deviates from unity, the higher will be the preferred orientation of $\text{Ga}_{0.03}\text{Zn}_{0.097}\text{O}$ thin films. The variation of texture coefficient estimated along (002) direction with annealing temperature of $\text{Ga}_{0.03}\text{Zn}_{0.097}\text{O}$ film is shown in Figure 5. It was found that the value of texture coefficient increases with increasing annealing temperature as shown in Table 3.

$$T_C(hkl) = \frac{I(hkl)/I_o(hkl)}{N_r^{-1} \sum I^{(hkl)}/I_o(hkl)} \quad (3)$$

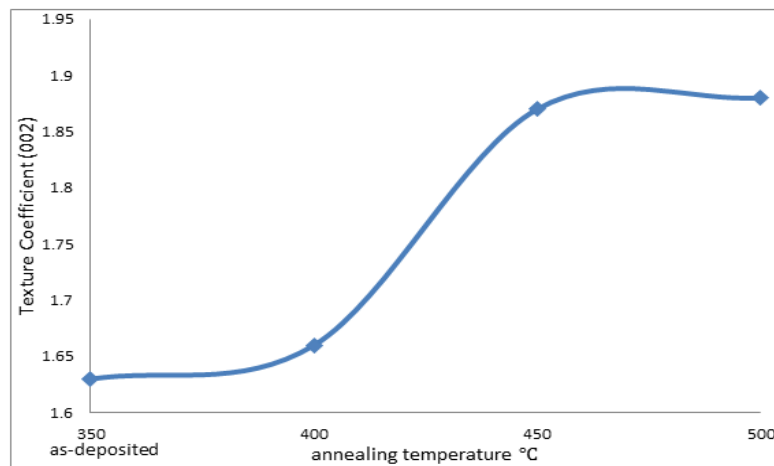


Figure 5 Texture coefficients vs. annealing temperature

The micro strain depends directly on the lattice constant (c) and its value related to the shift from the ASTM standard value. The values of micro strain of as-deposited and annealed $\text{Ga}_{0.03}\text{Zn}_{0.097}\text{O}$ films are listed in Table 3. This strain can be calculated from the following formula [34].

$$\langle \epsilon \rangle = \frac{|C_{ASTM} - C_{XRD}|}{C_{ASTM}} \times 100\% \quad (4)$$

The dislocation density (δ), defined as the length of dislocation lines per unit volume, has been estimated using the following equation [35], [36].

$$\delta = \frac{l}{D^2} \quad (5)$$

To derive the film stress (σ_{film}) parallel to the film surface, the following formula is used, which is valid for a hexagonal lattice [37].

$$\sigma_{film} = \frac{2c_{13}^2 - c_{33}(c_{11} + c_{12})}{2c_{13}} \times \frac{c_{film} - c_{bulk}}{c_{bulk}} \quad (6)$$

For the elastic constants c_{ij} , the following values for single crystal ZnO are used, $C_{11} = 208.8$ GPa, $C_{33} = 213.8$ GPa, $C_{12} = 119.7$ GPa, $C_{13} = 104.2$ GPa, Where: c_{film} and c_{bulk} are the lattice constants (c) of ZnO film and bulk (or powder).

Table 3: Structural properties of **Ga_{0.03}Zn_{0.097}O** film for different annealing temperature

Annealing temperature °C	Crystallite Size (nm)	Texture Coefficient T _c			Micro Strain ε %	Dislocation Density (δ) ($\frac{line}{m^2}$) $\times 10^{15}$	Film stress (GPa)
as-deposited 350	18.6	(101)	(100)	(002)	0.043	2.890	0.1001
400	21.8	0.633	0.731	1.63	0.093	2.104	0.2165
450	28.2	0.615	0.719	1.66	0.168	1.257	0.3911
500	30.6	0.551	0.577	1.87	0.179	1.067	0.4167

3.2. MORPHOLOGY

Figure 6 shows the AFM images of **Ga_{0.03}Zn_{0.097}O** samples as-deposited and annealed at 400, 450, 500 °C . As shown in the figure, the surface morphology changed with the varying annealing temperatures. For the as-deposited film the surface morphology was rough and rugged, and the root mean square (RMS) roughness of this film was 1.29 nm. This is attributed to the fact that the surface diffusion was insufficient due to the low deposition temperature [38]. However, after annealing the film at 400, 450, 500 °C under ambient atmosphere, the rough of the surface decreases with increasing annealing temperature up to 450°C and then it is increased for 500°C. The root mean square and grain size of **Ga_{0.03}Zn_{0.097}O** as-deposited and annealed have been listed in Table 4.

It is observed that, as the annealing temperature increased; the diffusion of atoms on the surface of glass substrate was enhanced, resulting in a flat or less rugged surface with (RMS) roughness 0.929 nm for the sample annealed at 450°C. Therefore it is concluded that the sufficient surface diffusion leads to the improvement of crystalline quality which accompanies the modification of the surface morphology.

Table 4: RMS roughness, Grain size and peak-peak height of **Ga_{0.03}Zn_{0.097}O** film

annealing temperature °C	RMS roughness (nm)	Grain size (nm)	Peak-Peak height (nm)
as-deposited 350	1.29	134.19	12.1
400	1.23	104.61	8.74
450	0.929	78.78	4.4
500	1.77	86.62	8.43

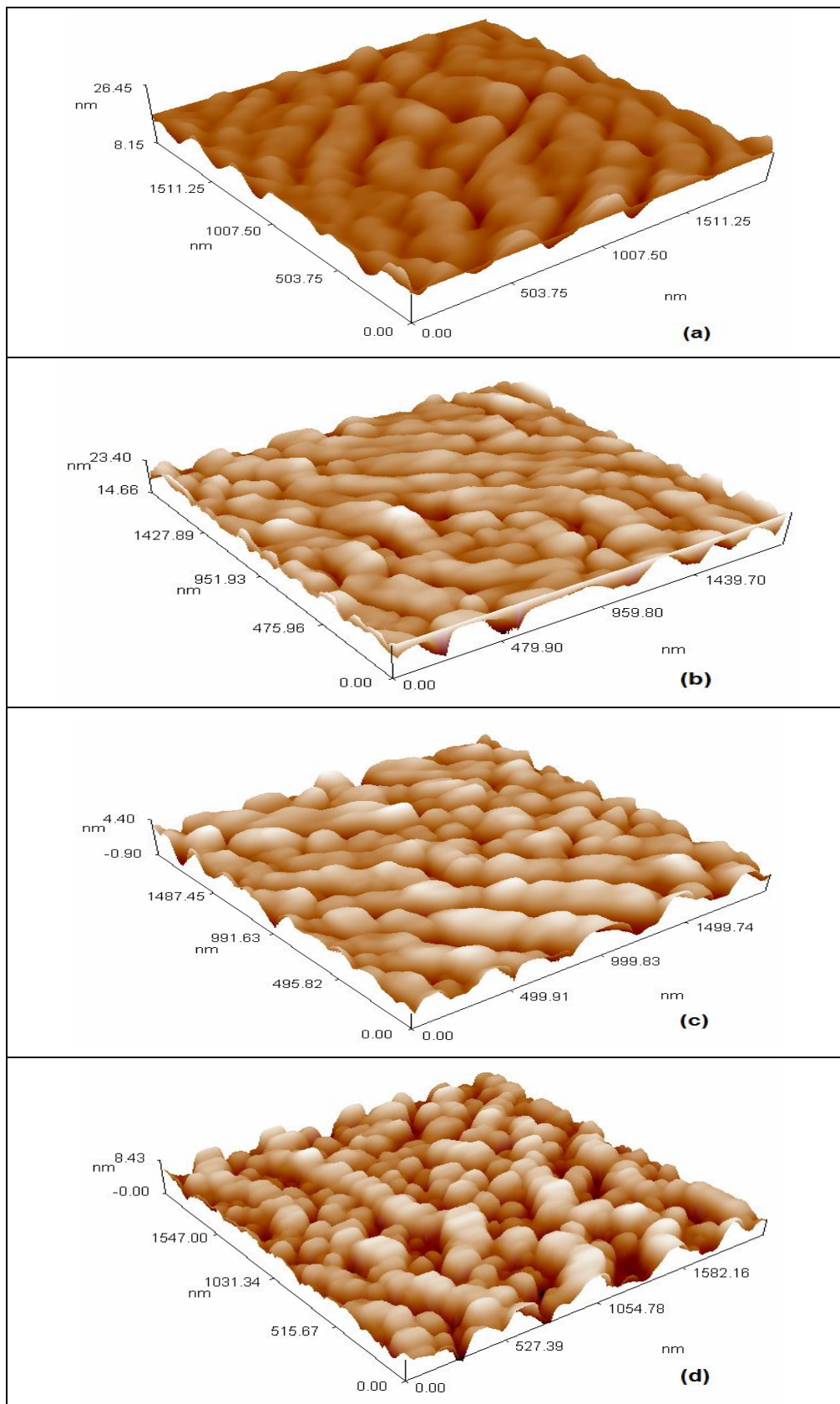


Figure 6 AFM images of $\text{Ga}_{0.03}\text{Zn}_{0.097}\text{O}$ thin film (a) as-deposited, (b) annealing at 400°C, (c) annealing at 450°C and (d) annealing at 500°C

3.3. OPTICAL PROPERTIES

Figure 7 shows the optical transmittance spectra taken at room temperature. The annealed $\text{Ga}_{0.03}\text{Zn}_{0.97}\text{O}$ films were highly transparent in the visible and IR regions from 400 to 900 nm and showed sharp absorption edge in the UV region. For the as-deposited film the transmittance is low compare with those of annealed films and no sharp absorption edge observed in this film. This indicates that the substrate temperature 350°C is not sufficient to arrange Ga and Zn ions sites in the lattice. We suggest that the band gap shift are directly proportional to the Ga ions which are substituted for the Zn ions in the film without changing the wurtzite structure, and at low deposition temperature, it is though that the Ga atoms are not incorporated in the ZnO lattice and are partially located at defect sites such as interstitials in $\text{Ga}_{0.03}\text{Zn}_{0.97}\text{O}$ lattice. Furthermore, the as-deposited film was less transparent in the visible and IR regions than other annealed films and the transparency of the films improved as the annealing temperature increased up to 450°C and then it decreases for further increasing in annealing temperature at 500°C . The decrease in the transmittance for the film annealed at 500°C can be described by the decreasing Ga content as a result of the increasing of re-evaporation rate of Ga atoms from the $\text{Ga}_{0.03}\text{Zn}_{0.97}\text{O}$ film [31].

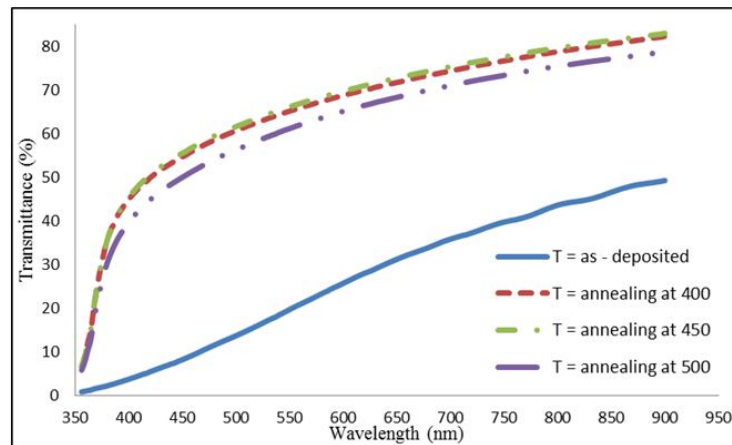


Figure 7 Transmittance spectra of $\text{Ga}_{0.03}\text{Zn}_{0.97}\text{O}$ film at different annealing temperature

The absorbance spectra of the $\text{Ga}_{0.03}\text{Zn}_{0.97}\text{O}$ thin film deposited on glass substrate at as-deposited and different annealing temperature that measured at room temperature is shown in Figure 8. In the high energy spectral range, where the film is strongly absorbent, and the absorbance of $\text{Ga}_{0.03}\text{Zn}_{0.97}\text{O}$ films decrease with increasing of annealing temperature from, 350°C (as-deposited) to 450°C , then it goes on increases with increasing substrate temperature from 450°C to 500°C .

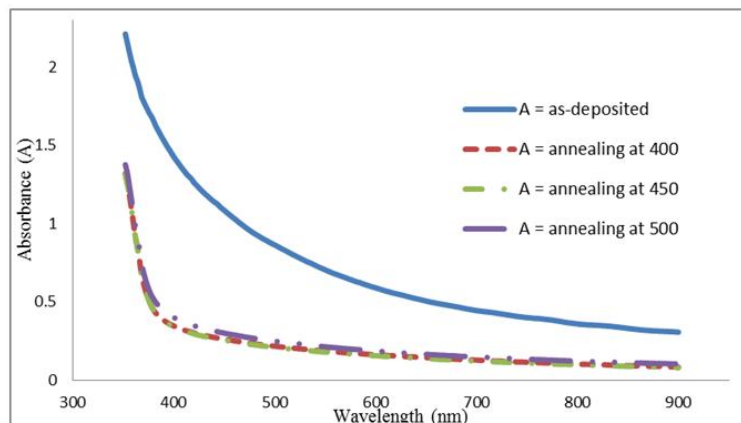


Figure 8 Absorbance spectra of $\text{Ga}_{0.03}\text{Zn}_{0.97}\text{O}$ film at different annealing temperature

The variation of absorption coefficient against photon energy $h\nu$ for direct band-to-band transition has the form: $Ah\nu = A(h\nu - E_g)^x$ where $h\nu$ is the photon energy, E_g is the band gap, A is the edge parameter. The value of x is $(1/2)$ for direct allowed transitions and (2) for indirect allowed transition. The films prepared in the present study have direct allowed transitions. Hence plots have been made by taken $(h\nu)$ along x-axis and $(ah\nu)^2$ along y-axis as shown in Figure 9.

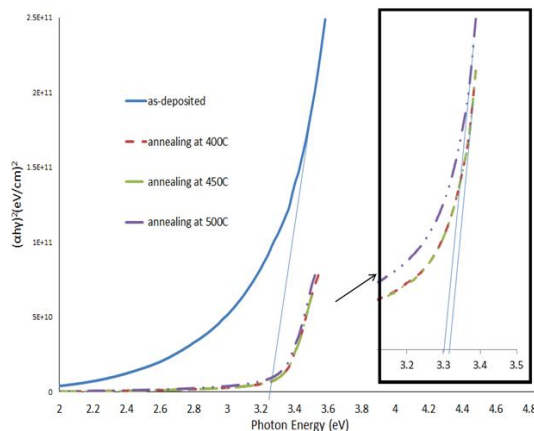


Figure 9 Variation of $(\alpha h\nu)^2$ vs. photon energy $(h\nu)$ of $\text{Ga}_{0.03}\text{Zn}_{0.97}\text{O}$ thin film

The values of direct band gap are estimated from the extrapolated of the linear portion of the curve to zero absorption and found to be (3.25, 3.32, 3.32, 3.3) eV for the as-deposited and annealed $\text{Ga}_{0.03}\text{Zn}_{0.97}\text{O}$ film at 400,450,500°C respectively, which are in agreement with the report [27]. From Figure 9 we can see that the bandgap of $\text{Ga}_{0.03}\text{Zn}_{0.97}\text{O}$ thin film increases with increasing annealing temperature from (3.25 eV) at as-deposited 350°C to (3.32 eV) at annealing temperatures 400, 450 °C and, then it decreases with increasing annealing temperatures from (3.32 eV) to (3.3 eV) at annealing temperatures 500°C.

4. CONCLUSION

$\text{Ga}_{0.03}\text{Zn}_{0.97}\text{O}$ thin films have been deposited successfully onto glass substrates at 350 °C by spray pyrolysis technique. The full width at half maximum (FWHM) value decreases from 0.4472 to 0.2717⁰ with increasing annealing temperature indicating the improvement of the crystalline quality of $\text{Ga}_{0.03}\text{Zn}_{0.97}\text{O}$ film. The crystalline quality of the films depends strongly on the annealing temperature due to the enhanced surface diffusion that comes with increasing annealing temperature.

The surface morphology changed with the varying annealing temperatures. The surface morphology of as-deposited film was rough and rugged because the surface diffusion was insufficient due to the low deposition temperature. However, after annealing the film, the rough of the surface decreases with increasing annealing temperature up to 450 °C and then it is increased at 500 °C. As the annealing temperature increased, the diffusion of atoms on the surface of glass substrate was enhanced, resulting in a flat or less rugged surface with (RMS) roughness 0.929 nm for the sample annealed at 450°C. Therefore it is concluded that the sufficient surface diffusion leads to the improvement of crystalline quality which accompanies the modification of the surface morphology.

For the as-deposited film the transmittance is low compare with those of annealed films and no sharp absorption edge observed in this film. This indicates that the substrate temperature 350 °C is not sufficient to arrange Ga and Zn ions sites in the lattice. At low deposition temperature, it is thought that the Ga atoms are not incorporated in the ZnO lattice and are partially located at defect sites such as interstitials in $\text{Ga}_{0.03}\text{Zn}_{0.97}\text{O}$ lattice. Furthermore, the as-deposited film was less transparent in the visible and IR regions than other annealed films and the transparency of the films improved as the annealing temperature increased up to 450 °C and then it decreases for further increasing in annealing temperature at 500 °C. The decrease in the transmittance for the film annealed a 500 °C can be described to the decreasing Ga content as a result of the increasing of re-evaporation rate of Ga atoms from the film.

References

- [1] K. Postava, H. Sueki, M. Aoyama, T. Yamaguchi, C. Ino, Y. Igasaki, M. Morie, J. Appl. Phys. 87 (2000) 7820.
- [2] C. Kwon, H. Hong, D. Yun, K. Lee, S. Kim, Y. Roh, B. Lee, Sens. Actuators B. 25 (1995) 610.
- [3] S. Major, S. Kumar, M. Bhatnagar, K. Chopra, Appl. Phys. Let. 49 (1986) 394.
- [4] M. Ambia, M. Islam, M. Hakim, J. Mater. Sci. 27 (1992) 5169.
- [5] K. Mukae, K. Tsuda, I. Nagasawa, Jpn. J. Appl. Phys. 16 (1977) 1361.
- [6] S. Chang, Y. Su, Y. Shei, J. Vac. Sci. Technol. A 13 (1995) 385.
- [7] T. Minami, T. Miyata, Y. Ohtani, T. Kuboi, Phys. Stat. Sol. (RRL) 1 (2007) R31.
- [8] R. Cebulla, R. Wendt, K. Ellmer, J. Appl. Phys. 83 (1998) 1087.
- [9] K. Iwata, T. Sakemi, A. Yamada, P. Fons, K. Awai, T. Yamamoto, S. Shirakata, K. Matsubara, H. Tampo, K. Sakurai, S. Niki, Thin Solid Films 480-481 (2005) 199.
- [10] T. Yamada, A. Miyake, S. Kishimoto, H. Makino, N. Yamamoto, T. Yamamoto, Appl. Phys. Let. 91 (2007) 051915.

- [11] A. Agura, A. Suzuki, T. Matsushita, T. Aoki, M. Okuda, *Thin Solid Films* 445 (2003) 236.
- [12] J. Steinhäuser, S. Fay, N. Oliveira, E. Vallat-Sauvain, C. Ballif, *Appl. Phys. Lett.* 90 (2007) 142107.
- [13] A. Reddy, P. Prathap, Y. Subbaiah, K. Reddy, J. Yi, *Thin Solid Films* 516 (2008) 7084-7087.
- [14] S. A. Yousif, A. A. Rasheed, N. F. Habubi, *Journal of Electron Devices*, 16(2012), 1347-1355
- [15] S. J. Pearton, D. P. Norton, K. Ip, W. Y. Heo, T. Steine, *Prog. Mater. Sci.* 50 (2005) 293.
- [16] Q. B. Ma, Z. Z. Ye, H. P. He, L. P. Zhu, J. R. Wang, B. H. Zhao, *Mater. Lett.* 61 (2007) 2460.
- [17] G. Frank, E. Kauer, H. Kostlin, *Thin Solid Films* 77 (1981) 107.
- [18] Q. B. Ma, Z. Z. Ye, H. P. He, L. P. Zhu, J. Y. Huang, Y. Z. Zhang, B. H. Zhao, *Scr. Mater.* 58 (2008) 21.
- [19] F. Q. Adurodiya, H. Izumi, T. Ishihara, H. Yoshioka, H. Matsui, M. Motoyama, *Jpn. J. Appl. Phys.* 38 (1999) 2710.
- [20] R. Das, S. Ray, *J. Phys. D: Appl. Phys.* 36 (2003) 152.
- [21] S. J. Henley, M. N. R. Ashfold, D. Cherns, *Surf. Coat. Technol.* 177 (2004) 271.
- [22] Q. B. Ma, Z. Z. Ye, H. P. He, S. S. Hu, J. R. Wang, L. P. Zhu, Y. Z. Zhang, B. H. Zhao, *J. Cryst. Growth*. 304 (2007) 64.
- [23] V. Assuncao, E. Fortunato, A. Marques, H. Aguas, I. Ferreira, M. E. V. Costa, R. Martins, *Thin Solid Films* 427 (2003) 401.
- [24] Q. B. Ma, Z. Z. Ye, H. P. He, L. P. Zhu, Y. Z. Zhang, B. H. Zhao, *J. Inorg. Mater.* 22 (2007) 1113.
- [25] Joint Committee on Powder Diffraction Standards, *Powder Diffraction File*, International Center for Diffraction Data, Swarthmore, PA (1997) card 36-1451
- [26] W. T. Yen, Y. C. Lin, P. C. Yao, J. H. Ke, Y. L. Chen, *Thin Solid Films* xxx (2009) xxx-xxx
- [27] A. R. Babar, P. R. Deshamukh, R. J. Deokate, D. Haranath, C. H. Bhosale, K. Y. Rajpure, *J. Phys. D: Appl. Phys.* 41 (2008) 135404 (6pp).
- [28] A. Ohtomo, M. Kawasaki, T. Koida, K. Masubuchi, H. Koinuma, Y. Sakurai, Y. Yoshida, T. Yasuda, Y. Segawa, *Appl. Phys. Lett.* 72 (1998) 2466.
- [29] W. Park, G. Yi, H. Jang, *Appl. Phys. Lett.* 79 (2001) 2022.
- [30] T. Minemoto, T. Negami, S. Nishiwaki, H. Takakura, Y. Hamakawa, *Thin Solid Films* 372 (2000) 173.
- [31] D. Hwang, M. Jeong, J. Myoung, *Appl. Surf. Sci.* 225 (2004) 217-222.
- [32] A. Goswami, *Thin Film Fundamentals*, New Age International (P) Ltd. Publishers, New Delhi, (2005) 69.
- [33] S. A. Yousif, J. M. Abass, *International Letters of Chemistry, Physics and Astronomy* 13(2013) 90-102.
- [34] T. Obata, K. Komeda, T. Nakao, H. Ueba, and C. Tasygama, *J. Appl. Phys.*, 81, (1997), 199.
- [35] V. Bilgin, S. Kose, F. Atay, I. Akyuz, *Mater. Chem. Phys.* 94 (2005) 103.
- [36] S. Prabakar, M. Dhanam, *J. Cryst. Growth* 285 (2005) 41.
- [37] R. Hong, J. Huang, H. He, Z. Fan, J. Shao, *Appl. Surf. Sci.* 242 (2005) 346-352.
- [38] B. Li, Y. Liu, Z. Zhi, D. Shen, Y. Lu, J. Zhang, X. Kong, X. Fan, *Thin Solid Films* 414 (2002) 170.